Available online at www.sciencedirect.com
ScienceDirect
Cement and Concrete Research 36 (2006) 1969–1984
Cement and Concrete Research

Influence of the age and drying process on pore structure and sorption isotherms of hardened cement paste

Rosa Maria Espinosa *, Lutz Franke

Department of Building Physics and Building Materials, Hamburg University of Technology, Eißendorfer Strasse 42, 21071 Hamburg, Germany

Received 7 February 2005; accepted 28 June 2006

Abstract

Sorption isotherms and scanning-isotherms of hardened Portland cement paste were measured. A structure model was developed to give a theoretical interpretation for the measured sorption isotherms. In particular, the causes for hysteresis between adsorption and desorption were described. Not only the capillary effect between condensation and evaporation in the pores but also the chemical water uptake, the drying method and the chemical aging have to be considered to explain the significant hysteresis. These results are the basis of our model for the structure and the porosity change of cementitious materials. The mathematical implementation of the structure model (called IBP-method [R.M. Espinosa, Sorptionsisothermen von Zementstein und Mörtel, Dissertation Hamburg University of Technology, 2004.]) will be described in a further essay [R.M. Espinosa, L. Franke, Inkbottle Pore-Method: prediction of hygroscopic water content in hardened cement paste at variable climatic conditions, Cement and Concrete Research (2006-this issue) doi:10.1016/j.cemconres.2006.06.011].

Keywords: Adsorption; Desorption; Hysteresis; Change of pore structure; Inkbottle pores

1. Introduction

The adsorption and desorption isotherms are necessary in order to predict the hygroscopic water content in cementitious materials at changing climatic conditions. Since hysteresis between adsorption and desorption isotherms is very significant, the (not trivial) paths between the sorption isotherms, frequently called “scanning isotherms”, must also be known.

Sorption thermodynamics and the particular pore structure of cementitious materials determine the sorption behaviour. Since the pore structure changes during the cement hydration [18], the drying-process [8,35] and the chemical aging [32,33], it can be expected that they also affect the sorption behaviour.

In this section the general sorption theory and the most important theories about the change of the structure of hcp, when submitted to changes of humidity, will be described shortly. Some aspects of these theories were used for the development of the own structure model.

In Section 2 the used materials and the experiments will be described. In Section 3 some experimental results of sorption isotherms and scanning-isotherms will be shown and discussed. The goal of this work was the development of an own structure model for hardened cement paste to explain its sorption behaviour. Hereby, the sorption hysteresis is affected considerably by the formation of inkbottle pores. The developed structure model will be described in Section 4 and then used in Section 5 to detail all reasons for hysteresis behaviour.

1.1. Backgrounds on sorption behaviour of hardened cement paste

Since the beginning of the 20th century (Langmuir [6]) a lot of works about sorption isotherms have been published worldwide. Thus the sorption mechanisms, i.e. (molecular) adsorption, capillary condensation and capillary evaporation, can be regarded as fundamentally well known.

Gibbs deduced a thermodynamical theory to explain the adsorption of gas molecules on a solid surface, the well-known “Surface Thermodynamics”. Thus Gibbs [19] deduced the equation for free adsorption, called “Gibbs adsorption isotherm”. “Excess surface properties“ are assigned to the surface

* Corresponding author. Tel.: +49 40 42878 2056; fax: +49 40 42878 2905.
E-mail address: espinosa@tuhh.de (R.M. Espinosa).

0008-8846/$ - see front matter © 2006 Published by Elsevier Ltd.
doi:10.1016/j.cemconres.2006.06.010

phase as the surface tension γ. Thereby the surface phase thickness is neglected.

According to Powers [26] and Bazant [7], Gibbs "Surface Thermodynamic" is appropriate to describe the adsorption in meso and macro pores, however the dependence of the surface tension on the surface phase thickness must be introduced.

The thermodynamic equilibrium between liquid and its vapour in a capillary leads to the relation between vapour pressure and capillary radius and thus to the theory of the capillary condensation [27,9,20]. Above this pressure vapour condensates (below saturation point) and the capillary is filled with liquid. Gibbs deduces the equilibrium between liquid and vapour using the "Surface Thermodynamics" theory. A satisfactory simplification is given by the well-known and very frequently used Kelvin equation [9].

The different liquid–vapour interface during capillary condensation and capillary evaporation leads to a pronounced *hysteresis* by simple pore geometries. Indeed some researchers came to the conclusion that the existence of so-called "inkbottle pores" causes a significant hysteresis between capillary condensation and evaporation.

There are various models to explain the *change of the microstructure* of the hardened cement paste, when hardened cement paste is submitted to changes of humidity.

Feldman and Sereda [16,17] explain hysteresis at very low relative humidity due to an irreversible uptake of interlayer water. Irreversible water fills the place between CSH-Phases and is bounded to solid under very high interaction forces. Thus the removal of irreversible water leads to a significant irreversible shrinkage, which points to an irreversible change of the microstructure of the CSH-Phases (Fig. 1).

The theory "Thermodynamics of hindered sorption" (based on Derjaguin [12]) is used to describe the water filling of micro gel pores (i.e. pore radius <1 nm). Surface tension and capillary pressure cannot explain the high interaction between micro gel pore water and solid. Indeed if the distance between the pore walls is smaller than 2.6 nm, an additional high interaction force between liquid film and solid is working. This is called disjoining pressure and depends only on the film thickness. Bazant [7] and Powers [26] affirm that the disjoining pressure and the capillary pressure determine the mechanical behaviour of cementitious materials and thus the change of the microstructure.

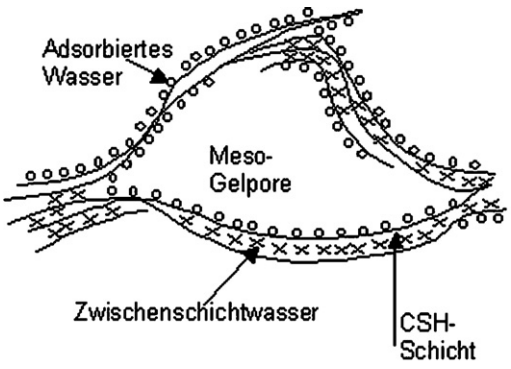

Fig. 1. Structure of cement gel according to Feldman.

However, according to the Munich model [28,34] the influence of the disjoining pressure in water-filled micro gel pores can be neglected. Swelling and shrinkage [35] of concrete are mainly due to the change of surface energy of the cement gel particles during adsorption and capillary condensation. Furthermore the Munich model allows to calculate the pore size distribution of the meso gel porosity by means of sorption isotherms. The well-known "thermodynamic approach" considers the dependence of the surface tension on the adsorption film thickness.

Finally, the measurement of sorption isotherms is a very long process. Thus it is necessary to develop computation methods for the prediction of the hygroscopic water content at changing climatic conditions. There are several correlation methods for the *computation of sorption* isotherms, i.e. in [21]. The necessary parameters have no physical meaning. They can only be calculated by fitting experimental results. So it is not possible to transfer them to materials with other properties. A further disadvantage of correlation methods is that further approximation parameters are required for the computation of desorption isotherm and scanning-isotherms.

Therefore it is necessary to develop a theoretical model for the calculation of the equilibrium water content at changing climatic conditions [3,4]. Our computation method is based on two methods – "excess surface work" and "disjoining pressure isotherm" according to Adolphs et al. [1,2,10]. Furthermore, our method extends them by using the experimental results discussed in the present paper. This new model will be presented in a following essay [15].

2. Material composition and experiments

Portland cement CEM I 42.5 R from two cement plants (designated as ZAB and ZA) was used for the experiments. The cement was mixed with water using the following water–cement ratios (w/c): 0.40, 0.50 and 0.60.

The hardened cement paste test pieces (4/4/16 cm^3) were stripped after 24 h and stored at 100% r.h. and 23 °C (curing storage conditions). At these conditions the pores are continuously water-filled and the cement hydratation can take place unhindered. Moreover, the carbonation of the material under these conditions is negligible even after several years.

The curing was stopped after 28 days (28d), 9 months (9Mon), 12 months (12Mon), 26 months (26Mon) and 3 years (3J), in order to obtain different hydration stages. Thus the influence of the cement hydration degree on pore structure and sorption behaviour could be analysed.

The material parameter "age" is set at the selected curing time (28 days old, 9 months old, etc). The cement hydration of young hardened cement paste (28d) can continue during the sorption experiments.

The following analysis of hardened cement paste and mortars were accomplished:

– *Measurement of the sorption isotherms including the scanning-isotherms* according to the exsiccator procedure (long-time measurement). Slices (5 mm) were used for this experiment. Two kinds of drying procedures were used: freeze-drying (freezing at −40 °C and drying at 1 Pa pressure,) and a weaker

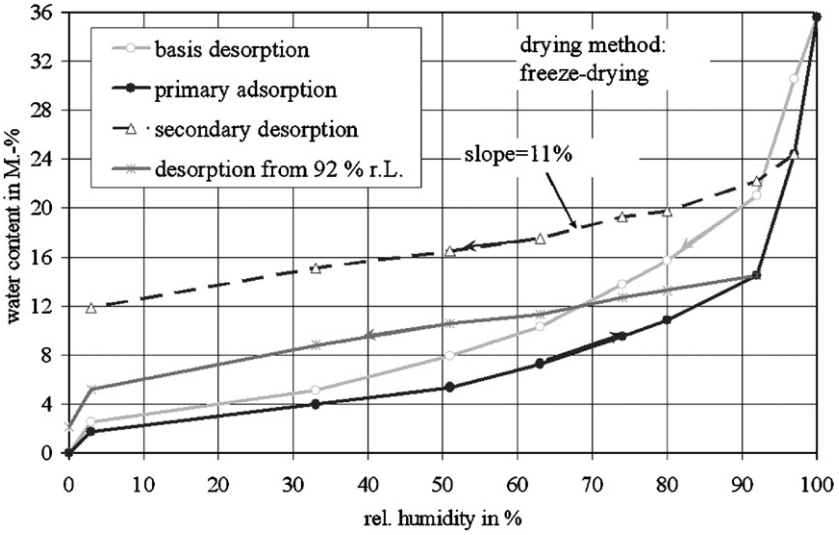

Fig. 2. Measured sorption isotherms of ZAB-28d w/c 0.60. Drying method: Freeze-drying.

drying-method, we called standard-drying (3% r.h. and 23 °C, that means, 84 Pa vapour pressure). Besides several short-time sorption measurements were conducted by means of a vapour sorption analysis instrument (IgaSorp).

- *Determination of the hydratation degree* with the help of the DTA/TG before and after the measurement of the sorption isotherms (in accordance with [18]).
- *Mercury intrusion porosimetry and nitrogen gas adsorption* for the characterisation of the pore size distribution before and after sorption. This allows the analysis of the change of the pore size distribution due to aging and drying at changing climatic conditions.

The ambient temperature was held constant at 23 °C during sorption experiments. The relative humidity was set constant at 3, 11, 33, 51, 63, 74, 80, 92 and 97% r.L.

The water content $w(\varphi)$ is defined as quotient between the weight change to each relative humidity and the dry weight of the porous material m_0:

$$w(\varphi) = \frac{m(\varphi) - m_0}{m_0} \times 100 \quad (1)$$

$m(\varphi)$ is the material weight to each relative humidity. Each sample series consisted of three samples, in order to determine variances of the material.

The samples were weighted once a week. It was assumed that the equilibrium was reached, when the change of the water content $w(\varphi)$ was less than 0.1% for two successive weeks. Therefore, the long-time measurement of the equilibrium moisture at each relative humidity took about 3 months, while the short-time measurements only 2 days. Obviously, the hydration of the hardened cement paste at the age of 28 days proceeds during the long-time sorption measurements.

In this case, the measured isotherms includes both physical and chemical adsorbed water, thus they are not exactly sorption isotherms. Nevertheless, this case is usual in practice, since the cement paste generally hydrates in situ during weathering by changing climate conditions.

On this account, the chemical water uptake during sorption has also to be accounted in our model (see Section 5.2) in case of young cement paste.

3. Sorption results and interpretation

The hygroscopic water content denotes the water content in porous materials due to adsorption and capillary condensation of water vapour (from air) in the material pores. Moisture transport can, however, lead to over-hygroscopic water content.

The exact transition point from hygroscopic into over-hygroscopic water content is difficult to define (according to literature it varies from 94% to 99% r.h.). In the following the transition between hygroscopic and over-hygroscopic water content is assumed to be 95% r.h. and is called *transition water content*. Above 95% r.h. capillary condensation and macroscopic condensation is presumed in capillary pores. Below 95% r.h. adsorption and capillary condensation set in gel pores.

3.1. Description of the main sorption isotherms

Fig. 2 exemplifies some sorption isotherms of hardened cement paste ZAB at the age of 28 days (ZAB-28d) and with w/c 0.60, which were measured according to the exsiccator method (DIN EN ISO 12571[1]).

The curing conditions were maintained constant at 100% r.h. and 23 °C. Thus material pores were continuously water-filled during curing. After 28 days the samples (5 mm × 40 mm × 40 mm) were stored into decreasing relative humidity at constant temperature (23 °C). The storage at the next lower humidity took place after reaching equilibrium.

Afterwards, the sample was dried to determine its reference weight (dry weight) m_0 by freeze-drying. The water content after the first desorption was calculated with Eq. (1). This first measured desorption is called basis desorption (see Fig. 2).

[1] DIN EN ISO 12571[2], German norm for the determination of hygroscopic sorption properties.

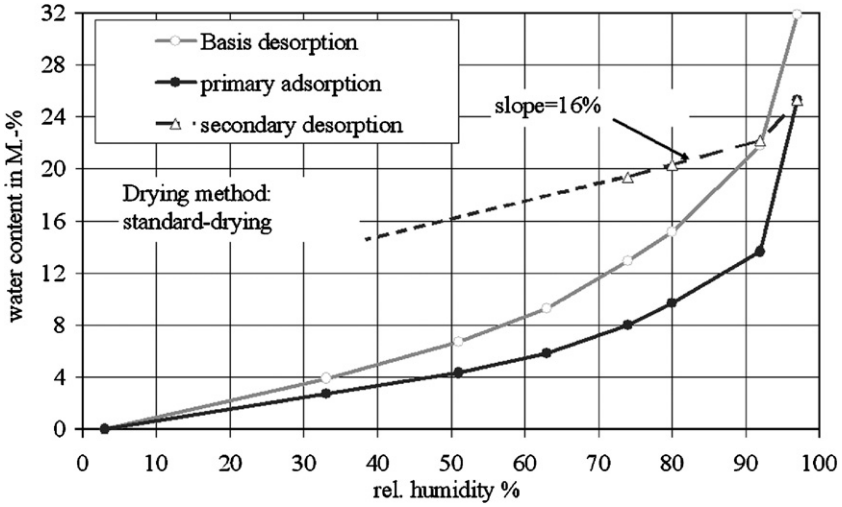

Fig. 3. Measured sorption isotherms of ZAB-28d w/c 0.60. Drying method: standard-drying.

After drying the sample was brought into increasing relative humidities for the measurement of the primary adsorption. Afterwards the secondary desorption and the desorption up to 92% r.h. were measured. Fig. 2 shows that secondary desorption and desorption from 92% r.h. are nearly parallel. Furthermore, the secondary desorption slope is equal to approximately 11%, clearly smaller than the slope of the basis desorption.

The significant difference between basis desorption and secondary desorption *points to a strong change of the pore structure*. The large amount of water that remains in material at 3% r.h. is worth to be noted (about 12 M.-%). Finally the sample was dried by means of freeze-drying and only 1 M.-% water remained in the material pores.

There is an additional difference between the basis desorption and the secondary desorption at 97% r.h. This is due to the complete saturation of the porosity during the curing process, just before the basis desorption was measured. Instead of this the water content at 97% r.h. at the beginning of the secondary desorption was only taken up by means of adsorption and capillary condensation. Hence only a small part of the capillary porosity is water-filled.

Fig. 3 shows the sorption isotherms of the hardened cement paste ZAB-28d w/c 0.60, when standard-drying is used instead of freeze-drying.

After standard-drying the secondary desorption exhibits a higher slope (16%) than after freeze-drying (11%). This means that the change of the pore structure is more pronounced by freeze-drying than by standard-drying (or by any other milder drying method).

A further chemical process that also causes a change of the microstructure of the hardened cement paste, is the so-called “chemical aging”. During chemical aging CSH phases tend to link with each other and this causes a compression of the cement gel particles. Strong drying accelerates this reaction, because this brings the CSH phases closer to each other and makes their cross-linking with each other easier.

In Section 4 it will be shown that cement hydration, drying and chemical aging cause the change of the pore structure of hardened cement paste.

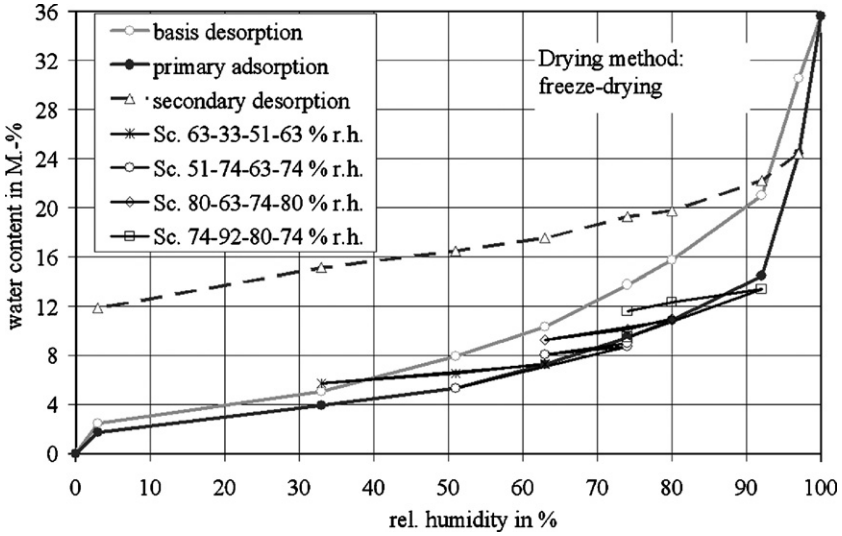

Fig. 4. Sorption isotherms and scanning-isotherms of ZAB-28d w/c 0.60 measured according to the exsiccator method. Drying method: freeze-drying.

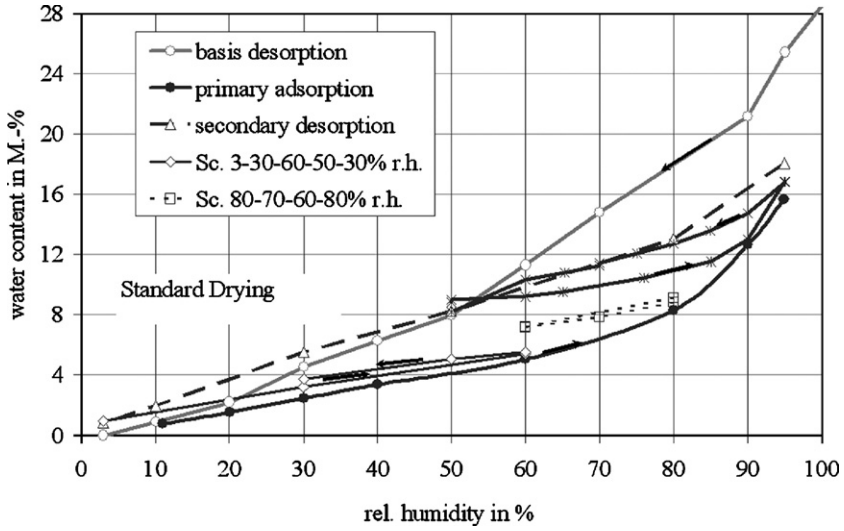

Fig. 5. Sorption isotherms and scanning-isotherms of ZAB-12Mon w/c 0.60 measured by means of IgaSorp. Drying method: standard-drying.

3.2. Scanning-isotherms of Portland hardened cement paste

Exemplary, Fig. 4 shows a selection of scanning-isotherms for hardened cement paste ZAB-28d w/c 0.60 after freeze-drying.

The diagram shows that:

- Basis desorption and secondary desorption are strongly different from each other (compare slopes).
- All scanning-isotherms run between primary adsorption and secondary desorption and are nearly parallel to the secondary desorption. This means that the change of the pore structure of all samples is similar even at different humidity conditions.
- The content of hydrate water (i.e. the hydration degree) before and after sorption measurements differs from each other. This means that the cement hydration after a curing time of 28 days has continued during the sorption measurements.

The scanning-isotherms in Fig. 5 were measured by means of IgaSorp (gravimetric analyser for measurement of vapour sorption by Hiden Analytical). The sample drying takes place in IgaSorp by 3% r.h. and 23 °C (standard-drying).

The equilibrium moisture is reached within 2 days due to the small sample mass (about 350 mg). That is about 30 times faster than by means of the exsiccator procedure (sample mass about 15 g). Thus the effect of time-dependent procedures such as carbonation, chemical aging and cement hydration is considerably less significant for the short-time measurements. Moreover the hardened cement paste was cured during 12 months (ZAB-12Mon), thus the cement hydration was approximately concluded.

Scanning-isotherms run between secondary desorption and primary adsorption also if the standard-drying process is used. The slope of the scanning-isotherms is higher than after freeze-drying.

Fig. 6 exemplifies the cyclic scanning-isotherm (80–97–3–51–80% r.h.) of a 3.5 years old hardened cement paste (with w/c 0.60). The cement hydration at this age is practically finished. The scored lines indicate that the water content between the measured points is unknown.

The scanning-isotherm is closed even though the measurements take several years. For example, the last measured water content by 80% r.h. (point 5) lies on the primary adsorption. This means, that the action of time-dependent processes such as carbonation, aging and hydration is negligible during the sorption measurement of this old hardened cement paste. The results are repeatable.

In conclusion, the change of the pore structure at changing humidity conditions has the same influence on the scanning-isotherms as on the secondary desorption (see Section 4).

4. Structure model for hardened cement paste

The sorption behaviour of a porous material is given by the *pore structure and by the interaction between matrix and water.* Indeed, the change of the pore structure due to the interaction forces caused by changing climatic conditions must be known for the correct prediction of the hygroscopic water content, which is the main goal of our work.

During the sorption measurements, the hydration of cement can proceed if enough water is contained in the capillary pores. The Powers-Model [26] will be used for the calculation of the porosity development during hydration.

Our structure model is based on the Munich model [28,34] and in [29] and completes it with the action of the disjoining pressure against the micro gel pore walls. Micro gel pores fill the space between the CSH-needles according to the last results about the structure of the CSH phases by Stark et al. [31]. The assumption of the disjoining pressure permits to explain some sorption results, as it will be shown in Section 5.

Furthermore, the pore model has to be extended to the presence of inkbottle pores to explain the high hysteresis at very low humidities.

4.1. Model for the pore structure

Firstly a pore classification will be made, which is suitable for the purposes of this work. Table 1 shows our own pore

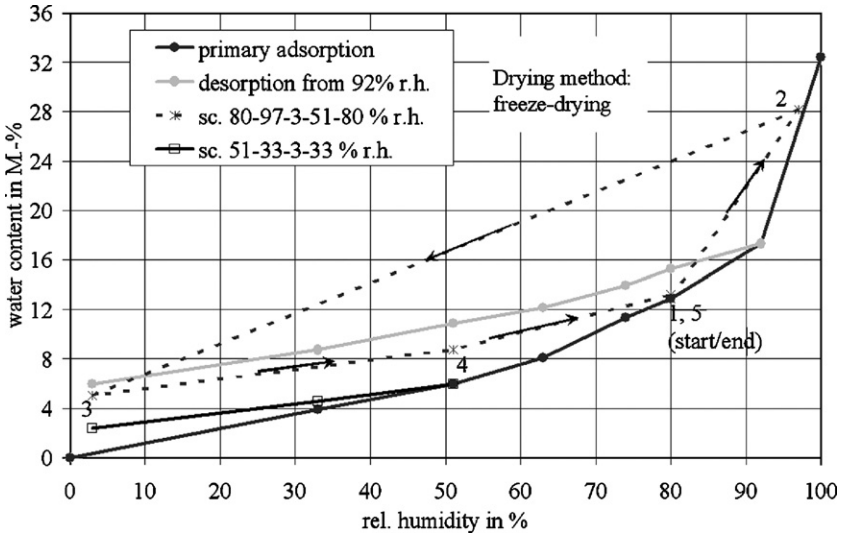

Fig. 6. Sorption isotherms and scanning-isotherms of ZAB, 3 years old with w/c 0.60 measured according to the exsiccator procedure. Drying method: Freeze-drying.

classification for cementitious materials. This classification agrees with the general classification according to IUPAC[2].

Our pore classification sets a *boundary between gel and capillary pores at 25 nm*. This assumption will be justified in the following.

According to Stark et al. [31] the CSH phases exhibit a needled X-ray-amorphous crystal structure (see Fig. 7a). The internal structure of the CSH needles could not be observed so far with ESEM-FEG (Environmental Scanning Electron Microscopy). Fig. 7b shows the pore model of hardened cement paste proposed by Jennings [36], which we will use to explain the hysteresis behaviour.

A boundary radius between gel and capillary porosity equal to 25 nm is assumed in order to describe the sorption behaviour using the pore size distribution measured by means of the mercury porosimetry [15]. In [36] it is shown that the area between the CSH needles constitutes the *gel porosity* ($R<25$ nm). The aggregation of CSH needles, which grow from the cement grains, mainly constitutes the cement gel particles. The *capillary pores* ($R>25$ nm) fill the space between the cement gel particles.

At nanometer scale it will be assumed that micro gel pores fill the small room between the CSH needles.

According to the model of Feldman [16], interlayer water corresponds to chemically bound water, which is taken up in the CSH-Phases during adsorption at low humidities. Interlayer water causes the change of the relationship $C_xS_yH_z$ and the increase of the density of the cement gel. According to this definition interlayer water is no pore water.

However, the available procedures do not permit to determine whether interlayer (hydrate) water or micro pore water is taken up and/or extracted from the material. This makes it impossible to distinguish between the adsorption of each of them. Therefore, in our work interlayer water is regarded as part of *micro gel pore water.*

[2] International Union of Pure and Applied Chemistry.

The porosity model was used to analyse the results of the mercury intrusion porosimetry. Thus, the porosity of hardened cement pastes at the ages of 28 days and 26 months was measured by means of mercury intrusion porosimetry and divided into gel pore and capillary pore volumes at the boundary radius (25 nm). The pore volumes were also computed according to the Hansen–Powers model [22] with the following constants: $a\times k=0.744$ [14] and $w_n^0=0.28$ g/g [18].

Fig. 8 shows computed (y axis) and measured (x axis) capillary pore volumes of ZAB-28d and ZAB-26Mon (26 months curing time), with w/c 0.40, 0.50 and 0.60.

The selected boundary radius between gel and capillary pores (25 nm) leads to a good correlation between measured and computed capillary pores content. However the mercury intrusion porosimetry underestimates the gel pore volume that is present according to the Hansen–Powers model. The difference is due to the fact that only pores larger than 1.8 nm can be measured, thus micro gel pores cannot be measured.

The total pore volume is determined by means of water uptake under vacuum and pressure followed by freeze-drying.

4.2. Interaction forces between water and hardened cement paste matrix

The developed structure model considers the following interaction forces:

– If pore surfaces are covered with an adsorbate (water film) and the pore radius is larger than 1 nm, the surface tension γ

Table 1
Own pore classification (in grew, meso pores from 1 to 50 nm)

Name	Hydraulic radius	Description
Gel pores	<1.0 nm	Micro gel pores
	1.0–25 nm	Meso gel pores
Capillary pores	25–50 nm	Micro capillary pores/meso capillary pores
	50 nm–1 μm	Macro capillary pores
	1 μm	

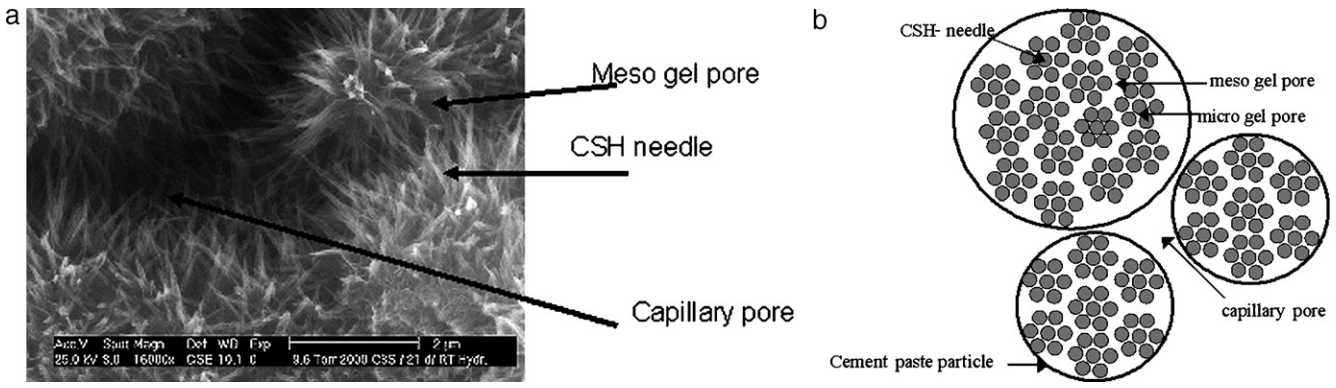

Fig. 7. a: C_3S after 21 days curing time, CSH-needles with diameter approx. 5 nm. b: Scheme of the pore structure of hardened cement paste [36].

of water has to be considered. The surface tension (or surface energy) decreases, if the thickness of the adsorbed water film grows, thus causing a decrease of the free energy of the system.

– If two parallel adsorbent walls carrying adsorbed water layers are closer than 2.6 nm, their mutual force interaction becomes noticeable. Thus, the water filling micro gel pores are submitted to the action of a strong spreading pressure Ω along the water film (stronger than the surface tension in case of adsorption in larger pores). This leads to the strong action of the disjoining pressure Π, the normal stress across the water film, which works against the pore walls. The disjoining pressure holds the pore walls at a constant distance procuring the stability of the system. Thus, the disjoining pressure avoids the collapse of the system.
– Finally, the capillary pressure acts on curved liquid films (by a radius of curvature smaller than approximately 50 nm).

According to the surface thermodynamics the free adsorption causes a change of the surface energy $\gamma \times d(A)$, which is the main reason for swelling and shrinkage during adsorption and desorption in the humidity range 3–40% r.h.

Capillary pores fill the space between gel particles (i.e. aggregation of CSH needles) and are larger than 50 nm according to our pore classification. Hence, in contrast to the Munich model the effect of the disjoining pressure between gel particles can be neglected. On the contrary, the action of the disjoining pressure has to be regarded in the micro gel pores, since the thickness of the contained water film is smaller than 1 nm.

The thermodynamics of hindered adsorption leads to the following relationship between disjoining pressure and surface energy of the thin film:

$$2\gamma(h) = 2\sigma - \int_{\infty}^{h} \Pi(h)\mathrm{d}h \qquad (2)$$

with σ the surface tension of the bulk liquid. Thus, the surface tension of the thin film depends on the thickness and on the disjoining pressure.

The disjoining pressure leads to a modified surface energy of the system compared to the free adsorption. Due to the removal of water from gel pores smaller than 2.6 nm the system becomes unstable, indeed. Since the disjoining pressure does no work against the CSH needles, an irreversible compaction of the cement gel takes place.

Therefore it will be regarded that the change of the total energy of hardened cement paste during adsorption and desorption is given by the action of all three interaction arts (surface tension, disjoining pressure and capillary pressure).

4.3. Remarks to the presence of inkbottle pores

Fig. 2 has shown the considerable difference between basis desorption and secondary desorption after freeze-drying. That points to a strong irreversible change of the pore structure, which can be explained as follows. Gel pores are enclosed by compressed cement gel after freeze-drying. Thus, they are only accessible through very small pores. However, a sufficiently strong drying process can extract the enclosed water content (e.g. by increasing the temperature or by means of freeze-drying). During climatic weathering a weaker drying has to be expected indeed. This leads to a smaller compression of cement gel.

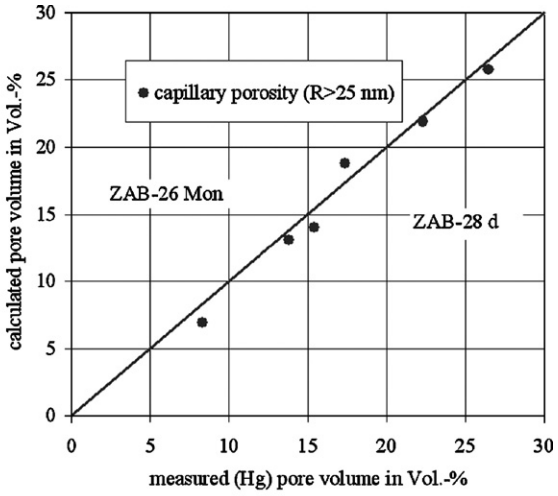

Fig. 8. Capillary pore volume measured by means of mercury intrusion porosimetry ($R>25$ nm) and computes according to the Hansen–Powers model with $a \times k = 0.744$ and $w_n^0 = 0.28$ g/g.

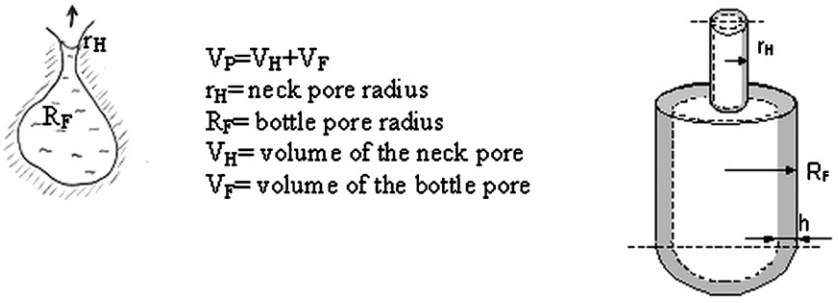

Fig. 9. Modelling inkbottle pores.

The compression of cement gel leads to coarsening of the pore structure, as it will be explained in Section 5.3. The sorption behaviour of the "new" meso gel porosity will be described by means of inkbottle pores.

Model inkbottle pores (see Fig. 9) are used for the mathematical modelling of the real pore system. Here bottle and neck pores are cylindrical and the bottom of the bottle pore is hemispherical.

The bottle pore with radius R_F is bounded to at least one neck pore with radius r_H ($r_H < R_F$).

The mathematical modelling of adsorption and desorption using inkbottle pores will be described in a further essay [15].

5. Description of the causes for the hysteresis of sorption isotherms

Micro pore filling, free adsorption in meso and macro pores and capillary condensation and capillary evaporation in meso pores are the sorption mechanisms in hardened cement paste.

Using a modified Kelvin equation, which considers the adsorbed film, a hysteresis between capillary condensation and capillary evaporation results depending on the pore geometry (see Section 5.1).

Finally, it must be considered that hardened cement paste is not an inert material. This means that chemical processes, which are not considered in sorption theories, can also be a reason for the sorption hysteresis. These will be described in Sections 5.2 and 5.3.

5.1. Hysteresis between capillary condensation and capillary evaporation

This classical kind of hysteresis is due to the different curvature of the interface adsorbate–vapour before capillary condensation and capillary evaporation. Additionally the interface curvature also depends on the pore geometry. This results in a different relative vapour pressure for capillary condensation and for capillary evaporation to each pore size.

According to the current knowledge about the structure and form of CSH phases (Fig. 7a), gel pores can be described as slit pores better than as cylindrical pores. Slit pores with closed ends lead to a complicated mathematical description of the relative vapour pressure by capillary condensation. So several simplifications of the pore geometry have to be assumed in order to calculate the vapour pressure.

Our own computation method (IBP-method [14,15]) leads to a satisfactory agreement with experimental results just assuming inkbottle pores and cylindrical pores. For this reason it is not necessary to model slit pores at this stage.

In the following hysteresis is deduced for cylindrical pores (with radius larger than 1 nm). The interaction between solid and adsorbate will be neglected at first (disjoining pressure). This is an acceptable assumption, since Π has a weak influence in pores larger than 1.5 nm compared to the effect of capillary pressure.

The classical model assumes that a cylindrical interface adsorbate–vapour builds up in cylindrical pores with two

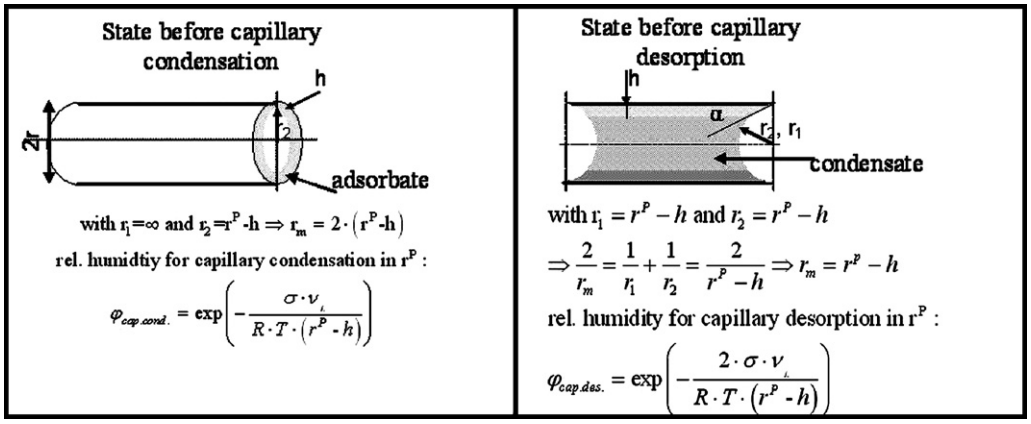

Fig. 10. Hysteresis of capillary condensation in cylindrical pores.

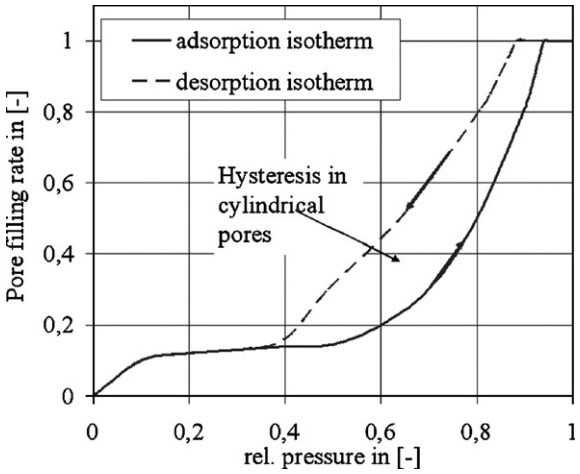

Fig. 11. Hysteresis between capillary condensation and desorption in cylindrical capillary pores.

opened sides, before capillary condensation takes place, while a hemispherical meniscus builds up at both pore sides before capillary evaporation starts (as shown by Fig. 10).

Thus it follows that capillary condensation and desorption begin in a certain pore radius at different vapour pressures or relative humidities. The resulting hysteresis is shown in Fig. 11.

Furthermore, Section 4.3 will show that inkbottle pores must be considered as part of the pore structure. The effective influence of inkbottle pores on sorption behaviour is described in a further essay [15].

5.2. Chemical water uptake during sorption

5.2.1. Influence of age and hydration degree

If enough capillary pore water is available during the sorption measurements, the cement hydration proceeds. Thus the hydration degree of hardened cement paste at the age of 28 days (ZAB-28d) increases during sorption at high relative humidity.

Experiments show that the influence of the age on the primary adsorption after standard-drying is practically negligible. Exemplary Fig. 12 shows the primary adsorption of hardened cement paste with w/c 0.60 at different ages.

In contrast, the effect of the age on the primary adsorption after freeze-drying is more significant. The water content shows the lowest value for the youngest hardened cement paste (ZAB-28d) (Fig. 13).

Above 33% r.h. the difference of water content in ZAB-28d and ZAB-12Mon remains almost constant (2.5 M.-%). This means:

- Pores that fill with water below 33% r.h., contain about 2.0 M.-% more water in ZAB-12Mon than in ZAB-28d. These pores are smaller than 1.5 nm (micro gel pores).
- The Powers model predicts an increase of gel pore water equal to 2.5 M.-% during hydration after 28 days until complete cement hydration.
- The difference between the primary adsorptions above 33% r.h. remains almost constant (≈2.0 M.-%). At 33% r.h. pores with radius equal to 1.5 nm fill with water. Thus meso gel porosity can be approximately regarded as independent of age (after 28 days curing time).
- Since micro gel pores remain water-filled after standard-drying, they do not participate in adsorption later. This explains the smaller influence of age on primary adsorption after standard-drying (Fig. 12) as compared to the freeze-drying process.

Table 2 gives the water content after standard-drying that remains in micro gel pores. It shows that the micro gel pore water increases by approximately 2.5 M.-% from 28 days curing time to 12 months.

These results confirm that micro gel pores are mainly formed during cement hydration after a curing period of 28 days.

5.2.2. Scaling of sorption isotherms according to hydration degree

New results are obtained if the water content is scaled over the ratio of hydrated hardened cement paste $x_{\mathrm{hydr.ZS,m}}$. This

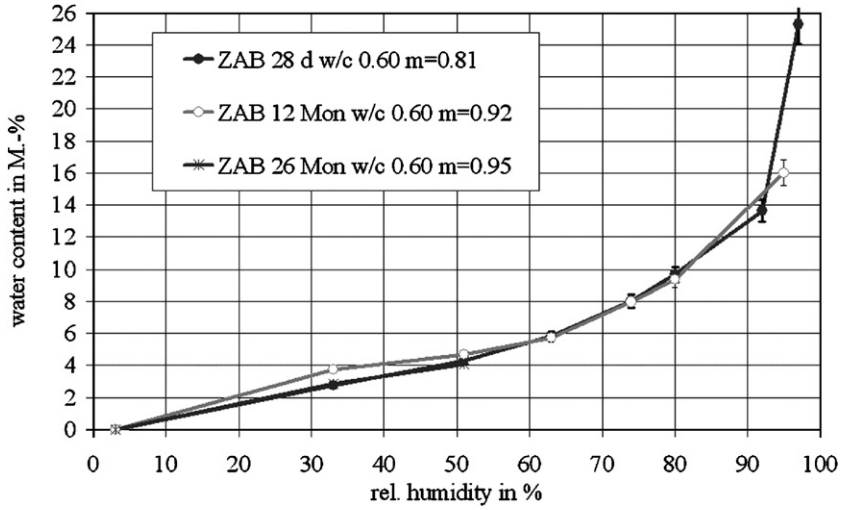

Fig. 12. Primary adsorption (after standard-drying) of Portland cement paste ZAB with w/c 0.60 at the age of 28 days, 12 months and 26 months.

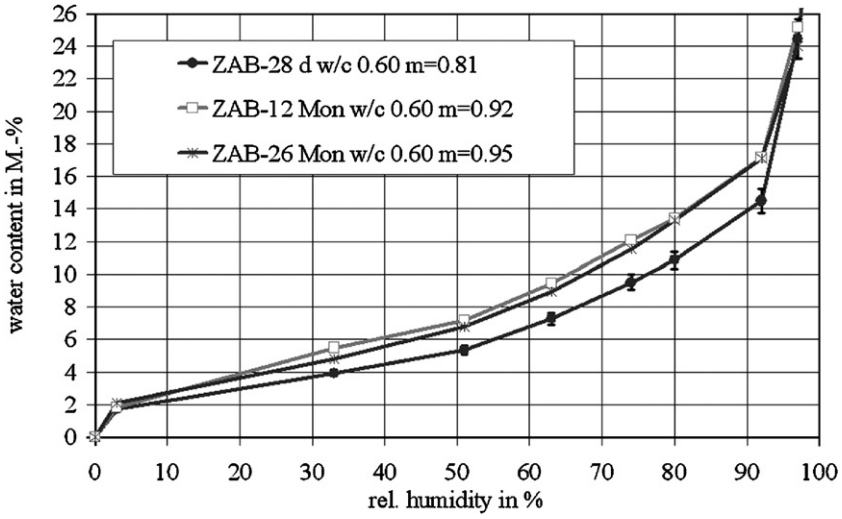

Fig. 13. Primary adsorption (after freeze-drying) of Portland hardened cement paste ZAB with w/c 0.60 after a curing time of 28 days, 12 months and 26 months.

can only be applied to the hygroscopic water content, which is taken up in cement gel (thus in gel pores). The hydration degree m and the maximum hydrate water content w_n^0 are necessary for the computation of the scaled hygroscopic water content $w_{\text{hydr.ZS}}$:

$$x_{\text{hydr.ZS,m}} = \frac{mc(1+w_n^0)}{c(1+mw_n^0)} \Rightarrow w_{\text{hydr.ZS}} = \frac{w}{x_{\text{hydr.ZS,m}}} \tag{3}$$

The empty small boxes in Fig. 14 give the scaled hygroscopic water content $w_{\text{hydr.ZS}}$ for ZAB-28d (x axis) and ZAB-12Mon (y axis).

The scaled hygroscopic water content $w_{hydr.ZS}$ lies on the diagonal. On the other side the non-scaled water content (filled circles) lies above the diagonal, since the hygroscopic water content of the older hardened cement paste is larger.

Thus, the difference between primary adsorption of ZAB-28d and ZAB-12Mon disappears by scaling:

$$w_{\text{hydr.ZS,28d}} = w_{\text{hydr.ZS,12Mon}} \text{ with } m_{28\text{d}} \neq m_{12\text{Mon}} \tag{4}$$

Besides it follows from Eq. (3) that the non-scaled hygroscopic water content is proportional to $x_{\text{hydr.ZS,m}}$:

$$w = w_{\text{hydr.ZS}}\, x_{\text{hydr.ZS,m}} \tag{5}$$

The ratio of hydrated hardened cement paste $x_{\text{hydr.ZS,m}}$ quantifies the influence of hydration degree on the hygroscopic water content. The scaling procedure cannot be applied to over-hygroscopic water content (contained in capillary pores), since capillary pore space is not proportional to the ratio of hydrated hardened cement paste.

Table 2
Remaining water content after standard-drying

Content of gel pore water after standard drying			
	w/c 0.40	w/c 0.50	w/c 0.60
ZAB-28d	2.5	2.4	2.5
ZAB-12Mon	4.3	4.2	5.1
ZAB-26Mon	4.0	4.1	5.0

5.2.3. Influence of dry mass on water content

The analysis by means of TG/DTA shows that the degree of hydration increases during sorption measurements. Thus the gel pore content increases and the hygroscopic water content with it.

As a result of the uptake of hydrate water the dry weight (m_0) also increases. The hydration degree before sorption measurements is equal to 0.7; during sorption measurements it increases to 1.0. The dry weight of hardened cement paste can be theoretically calculated as a function of the hydration degree m:

$$m_0 = c(1+mw_n^0)\begin{cases} m = 0,7 \Rightarrow m_{0,\text{D}-1} = 1,20c \\ m = 1,0 \Rightarrow m_{0,\text{D}-2} = 1,28c \end{cases} \tag{6}$$

The increase of the dry weight was confirmed by measuring the "new" dry weight after the secondary desorption. The water

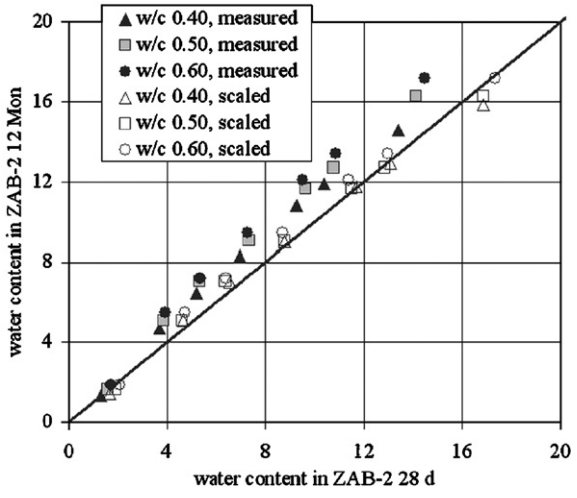

Fig. 14. Measured and scaled water contents (primary adsorption) of ZAB-12Mon and ZAB-28d after freeze-drying.

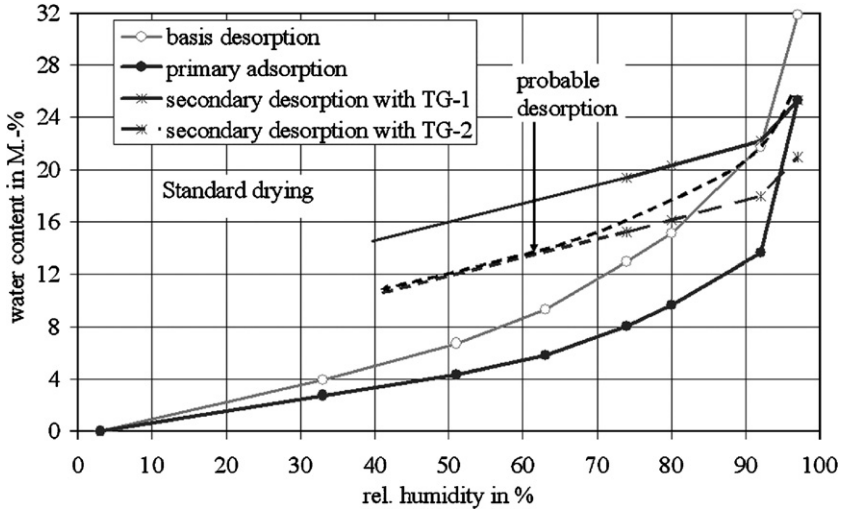

Fig. 15. Uncorrected and corrected secondary desorption with last dry weight (TG-2) obtained after sorption measurements. Material: ZAB-28d w/c 0.60. Standard-drying.

content was computed so far with the first dry weight of the samples. With the following equation it is possible to relate the water content to the new dry weight $m_{0,D.2}$:

$$w(\varphi)_{D.2} = w(\varphi)_{D.1}\frac{m_{0,D.1}}{m_{0,D.2}} - \frac{m_{0,D.2}-m_{0,D.1}}{m_{0,D.2}} \times 100 \qquad (7)$$

with

$$w(\varphi)_{D.1} = \frac{m(\varphi)-m_{0,D.1}}{m_{0,D.1}} \times 100 \text{ and}$$

$$w(\varphi)_{D.2} = \frac{m(\varphi)-m_{0,D.2}}{m_{0,D.2}} \times 100.$$

The result of this conversion is shown in Fig. 15.

– After drying the material samples were stored at 97% r.h. An equilibrium water content equal to 25 M.-% was taken up. This high pore water content enables the progression of cement hydration.
– Next the secondary desorption was measured. Hereby the samples were brought into gradually decreasing humidity.

The corrected secondary desorption lies below the uncorrected one (dotted line in Fig. 15). The influence of the new dry weight is clearly significant. Since chemical water binding takes place progressively during the storage, the real secondary desorption must lie between the dotted and the solid line. Thus the slope becomes larger. This correction was also used in Fig. 16.

The change of dry mass has only to be considered in case of young hardened cement paste.

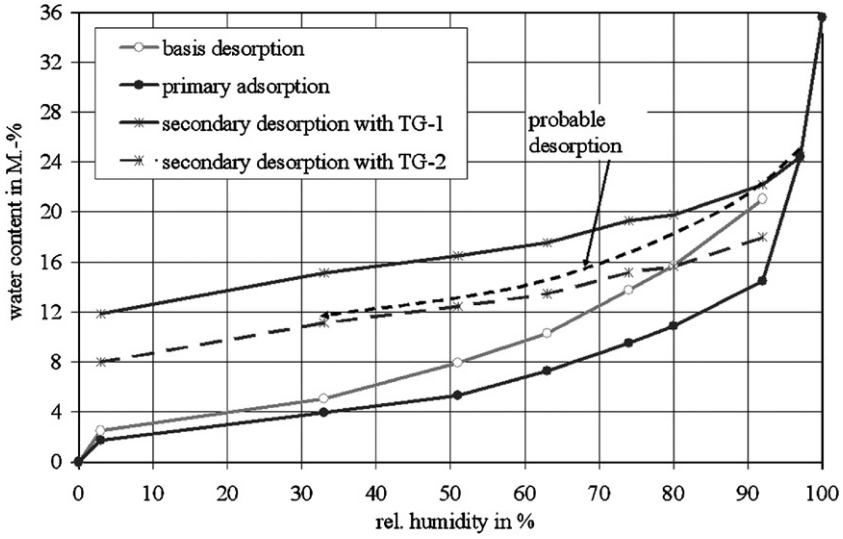

Fig. 16. Uncorrected and corrected secondary desorption with last dry weight (TG-2) obtained after sorption measurements. Material: ZAB-28d w/c 0.60. Freeze-drying.

5.3. Irreversible change of pore structure and formation of inkbottle pores

5.3.1. By use of laboratory drying methods

The water content $w(\varphi)$ is given as quotient of weight change and dry weight (m_0, reference weight) at each relative humidity according to Eq. (1).

Freeze-drying (1 Pa vapour pressure) and standard-drying (84 Pa vapour pressure) were used in this work to obtain the dry weights $m_{D-0\%}$ and $m_{D-3\%}$, respectively. Fig. 17 shows that the hygroscopic water content adsorbed after freeze-drying is considerably larger than after standard-drying.

However it must be considered that after standard-drying more water remains in the material pores than after freeze-drying. The remaining water content after standard-drying (Δm_0) can be computed with Eq. (8). The results were shown in Table 2:

$$\Delta m_0 = \frac{m_{D-3\%} - m_{D-0\%}}{m_{D-0\%}} \times 100 = \left(\frac{m_{D-3\%}}{m_{D-0\%}} - 1\right) \times 100$$

$$\text{and } \frac{m_{D-3\%}}{m_{D-0\%}} = \frac{w_{sat,D-0\%} + 100}{w_{sat,D-3\%} + 100} \text{ with } w_{sat,D} = \frac{m_{sat} - m_D}{m_D} \times 100$$

m_{sat} = Mass of saturated sample (in g)

w_{sat} = Water content at saturation (over D−3% or D−0%)

m_D = Dry mass (after D−3% or D−0%) (8)

Δm_0 varies from 2.5 to 5 M.-% depending on age and w/c and remains in pores with radius < 1.0 nm (i.e. in micro gel pores) in accordance to our pore size classification (see Table 1). The standard-drying process leads to a partial dried state evidently.

According to Eq. (1) a smaller dry weight leads to a higher water content $w(\varphi)$ at the same weight $m(\varphi)$. To investigate the influence of the drying method on sorption isotherm the water content must be referred to *the same reference weight*. The primary adsorption measured after standard-drying is converted by means of Eq. (9):

$$w(\varphi)_{D-0\%} = w(\varphi)_{D-3\%} \frac{m_{0,D-3\%}}{m_{0,D-0\%}} + \Delta m_0 \times 100 \text{ with } \frac{m_{0,D-3\%}}{m_{0,D-0\%}} = \Delta m_0 + 1 \quad (9)$$

The results are shown in Fig. 18.

Thus the water content after standard-drying ($w(\varphi)_{D-3\%}$) is related to the reference weight after freeze-drying $m_{0,D-0\%}$ (dotted line in Fig. 18).

The diagram shows that the absolute hygroscopic water content below 60% r.h. after freeze-drying is clearly smaller than after standard-drying. The largest difference results at 3% r.h., the freeze-drying leads indeed to a strong diminution of the water uptake below 3% r.h. That means that the micro gel porosity has significantly decreased due to the freeze-drying process.

The different adsorption behaviour points to a different pore structure. The *interaction forces* water–solid and solid–solid, which cause the change of the porosity, depend on the drying method and on its intensity:

- During the freeze-drying process the pore water (as ice) sublimates in meso and macro pores without the action of capillary pressure. Therefore a porosity change can be excluded.
- However micro gel water is existent not as ice but as liquid water during freeze-drying. By means of freeze-drying the water contained in the micro gel pores is extracted. For this reason the disjoining pressure does not work any more between the very close CSH needles. These become unstable and pull together causing a decrease of the micro gel porosity. Thus the removal of micro gel water leads to a very strong compression of the cement gel (usually called collapse of the CSH microstructure [8,33]). During this

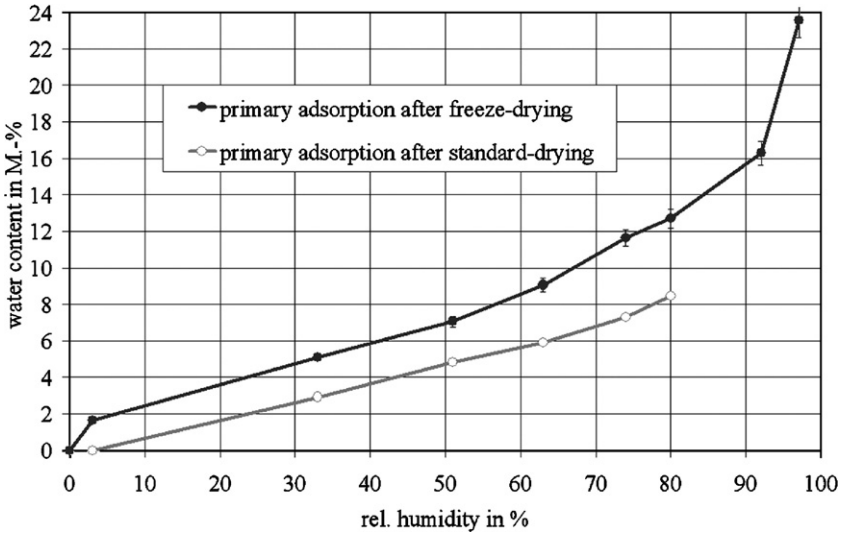

Fig. 17. Primary adsorption of ZAB-12Mon w/c 0.50. Drying methods: freeze-drying and standard-drying.

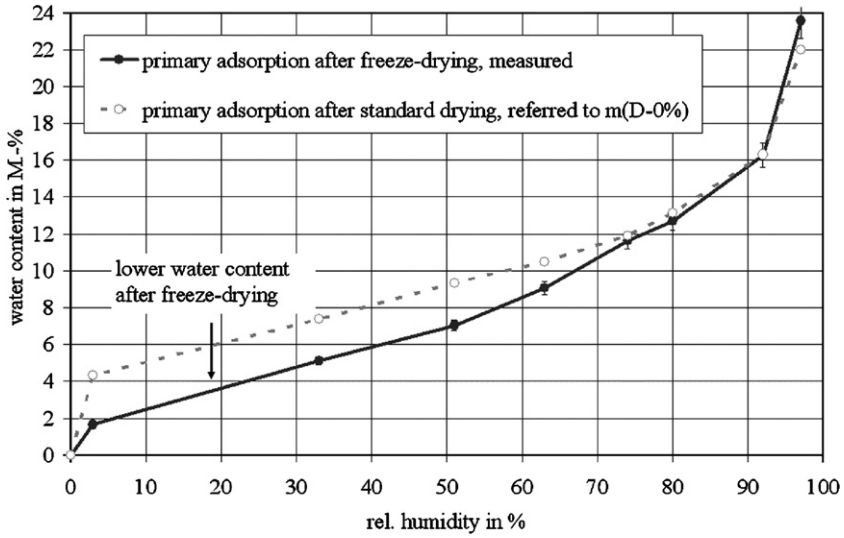

Fig. 18. Primary adsorption of ZAB-12Mon w/c 0.50 after freeze-drying and after standard-drying. Water content referred to $m_{D\text{-}0\%}$.

process some meso gel pores may be enclosed in the compressed cement gel, surrounded by collapsed CSH-needles. This yields a diminution of the open meso gel porosity too. Besides the volume of capillary porosity increases due to the compression of the cement gel. So the freeze-drying leads to a coarsening of the pore structure.

– In contrast to this, micro gel pores remain water-filled after standard-drying, However at this low humidity (3% r.h.) a partial gel compression takes also place. Firstly, the action of the disjoining pressure has to be regarded in pores smaller than approx. 2.6 nm. Since the standard-drying process dries a part of them (radius >1 nm), a partial collapse of the pore walls may occur. Secondly, the capillary pressure in the water-filled meso gel pores pull the pore walls together causing a compression of these pores. The analysis of the pore size distribution shows that the coarsening of the pore structure is less extensive than by freeze-drying (see Fig. 20).

A further sign for the partial irreversible change of the pore structure of hardened cement paste after freeze-drying is the reproducible *flat secondary desorption*. Here a high water content remains within the material (8 M.-% in Fig. 16 at approx. 3% r.h.). Only after sharper humidity reduction from 3% to approx. 0% (freeze-drying) pore water content is closer to 0 M.-%, so that a following secondary adsorption curve runs similar to the primary adsorption. A following tertiary desorption runs similar to the flat secondary desorption. Thus the described change of pore structure due to freeze-drying is irreversible.

By re-saturation after freeze-drying, the original water saturation content is reached. This shows that the overall porosity is still present. Other authors [33] consider this result as reversible change of the pore structure. In contrast the secondary desorption points to an irreversible change of the pore structure.

Fig. 5 showed that the secondary desorption after standard-drying runs closer to the basis desorption. The difference between basis desorption and secondary desorption is less pronounced after standard-drying (the slope of the secondary desorption is larger). The reason is the explained slighter compression of the cement gel during standard-drying.

These results were used to develop a structural model of hardened cement paste. Hereby the change of the gel porosity is described by a *formation of inkbottle pores* in the cement gel as follows:

– The amount of inkbottle pores is proportional to the intensity of the drying process.
– After drying some (bottle) pores are only accessible through very tiny (neck) pores after the compression of the cement gel. During the secondary desorption the material cannot be completely dried. The retained water content depends on the size of the neck pores and on the amount of the inkbottle pores.
– However a sufficiently strong drying process can extract the enclosed water (e.g. heating or freeze-drying).

5.3.2. Drying process at usual climatic conditions

The drying process during weathering is usually milder than the standard-drying process (84 Pa). Therefore the micro gel pores and a part of the meso gel porosity remain continuously water-filled. Beaudoin and Tamtsia [8] affirm that the microstructural change of CSH is influenced by the rate of drying, even by drying at an intermediate humidity (they say 79% r.h.). Feldman's measurements [16] show a length change of hardened cement paste over the whole humidity range also.

At an intermediate humidity the capillary pressure works in the water-filled pores pulling the pore walls together. By decreasing the relative humidity the intensity of the capillary pressure increases proportionally to $\log(\varphi)$ according to the Kelvin equation. This is the reason for the growing compression of the cement gel and coarsening of the pore structure at lower relative humidity.

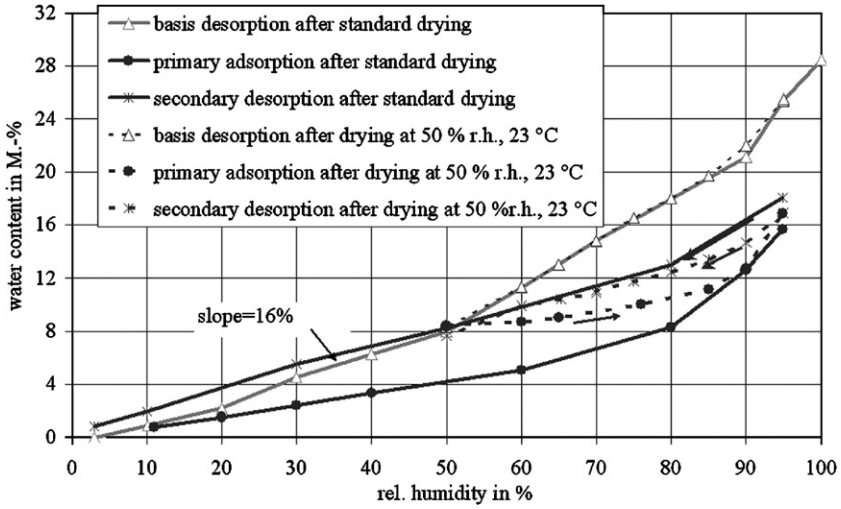

Fig. 19. Sorption isotherms of ZAB-12Mon w/c 0.60 measured with IGASorp. Drying Method: 50% r.h. and 23 °C and standard-drying.

The difference between basis and secondary desorption at 95% r.h. is due to the different saturation degree of the capillary porosity.

The whole pore structure is expected to be different because of the different drying intensity. Thus the coarsening of the pore structure is indeed more pronounced after standard-drying. However, Fig. 19 shows that the secondary desorption does not depend on the used drying process *in the common humidity range (>50 r.h.)*.

Moreover a chemical aging of the cement gel cannot be excluded during drying. This would lead to an irreversible change of the microstructure due to the polimerization of the CSH-phases. Hence, the change of the pore structure due to the chemical aging superposes to the change caused by drying. This will be explained in Section 5.3.4.

5.3.3. Analysis of the pore structure after drying

Water-saturated hardened cement paste samples at the age of 12 months were dried. Afterwards the pore size distribution was measured by means of mercury intrusion porosimetry (reference state). The next figure shows the different pore size distribution of ZAB-12 Mon W/Z 0.50 that results by freeze-drying and standard-drying (3% r.h. and 23 °C) (Fig. 20).

Moreover the mercury cannot fill the pores which are water-filled at 3% r.h. because they are smaller than the measurable pores.

By drying at 3% r.h the maximum of the pore size distribution is smaller and the pore surface larger (39.5 m^2/g vs. 35.1 m^2/g). As it was expected, the coarsening of the pore structure after freeze-drying is more significant due to the stronger compression of the cement gel.

By drying at 11% r.h. and at 33% r.h. it was proved that the higher the relative humidity used for drying is, the finer is the resulting pore size distribution.

It has to be remarked that the mercury intrusion porosimetry does not give any information about the micro gel porosity and the enclosed gel pores.

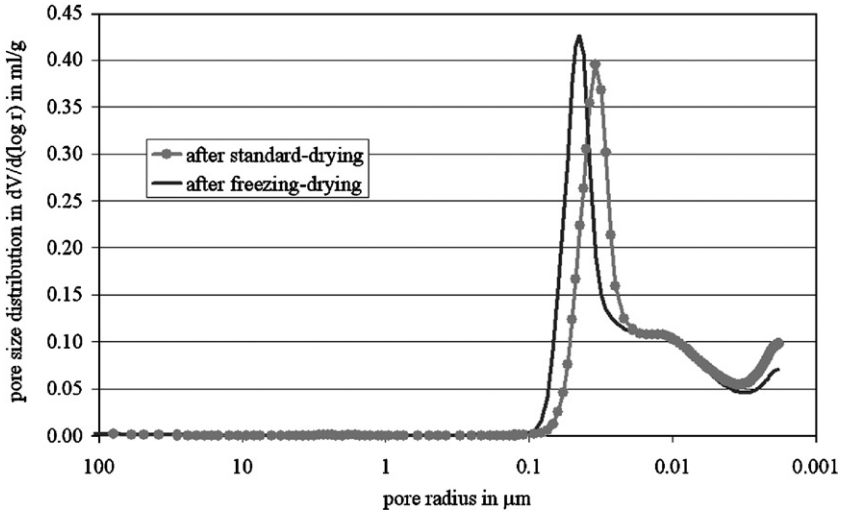

Fig. 20. Pore size distribution of ZAB-2 12Mon W/Z 0.50 by freeze-drying and by standard-drying (3% r.L. and 23 °C).

5.3.4. Irreversible change of hardened cement paste due to chemical aging

Carbonation and chemical aging are two different kinds of time-dependent processes that take place simultaneously during weathering. Both processes affect the pore structure and also the sorption behaviour.

Carbonation leads to a strong reduction of the pore volume and generally to a substantial reduction of water content uptake. Our analysis shows, however, that the carbonation of all used samples is negligible. Thus, the influence of carbonation on pore structure and on sorption behaviour will not be analysed and discussed in this essay.

A further chemical process that also causes a change of the microstructure of the hardened cement paste, is the so-called "chemical aging" (see definition in Section 3.1). Chemical aging takes place gradually causing a completely irreversible change of the pore structure due to the *compression of the cement gel particles* [25,32,33].

In our laboratory the dried material samples were exposed to changing humidity conditions for several years in order to measure some scanning-isotherms. After this long storage time a considerable chemical aging was expected according to [32,33].

The analysis of the pore structure change was carried out by means of mercury intrusion porosimetry and water uptake under pressure. Fig. 21 exemplifies the change of gel and capillary porosity of ZAB-28d w/c 0.60 related to the state in the reference state (directly after 28 days curing time). Both the decrease of the gel pore volume and the increase of the capillary pore volume suggest a substantial coarsening of the pore structure.

Furthermore, the reduction of the gel pore volume is larger than the increase of the capillary pore area, so that the measurable pore volume decreased (5% to 10%). Moreover *the total pore volume measured by means of water uptake under pressure remains approximately constant*.

This suggests that small gel pores are still present, but are not part of the measurable porosity by means of mercury intrusion porosimetry. That means that after chemical aging some gel pores become either too small to be measured or are enclosed by micro pores. Analogous to the findings in Section 5.3.1, the change of gel porosity can be described by a formation of inkbottle pores with very small neck pores. This is the basis for the mathematical description of the sorption behaviour when chemical aging takes place.

6. Conclusions

Adsorption, desorption isotherms and scanning-isotherms of Portland hardened cement paste were measured in the laboratory. Two drying methods were used to gel the dry mass (i.e. reference mass): freeze-drying (1 Pa) and standard-drying (84 Pa, 23 °C, 3% r.h.). The obtained hysteresis between adsorption and desorption is very significant, even by drying at usual climatic conditions.

Thus, sorption hysteresis has to be considered for the proper prediction of the hygroscopic water content, which is the goal of our investigations.

A structure model for hardened cement paste was deduced from the experimental and theoretical results in order to explain theoretically the significant hysteresis of the sorption behaviour. Not only the capillary effect between condensation and evaporation in the pores according to the well-known Kelvin equation but also the chemical water uptake, the drying process and the chemical aging have to be considered to explain the particular sorption behaviour of hardened cement paste.

The difference between the secondary desorption and the basis desorption reveals an irreversible change of the pore structure due to the drying process. In particular the freeze-drying process (commonly used in laboratories) causes a significant compression of the cement gel. This yields a formation of large amounts of inkbottle pores. The small radius of the ink pores is the reason for the large amount of water that remains in the pores close to 0% r.h. (approx. 11 M.-%). Thus the slope of the secondary desorption mainly

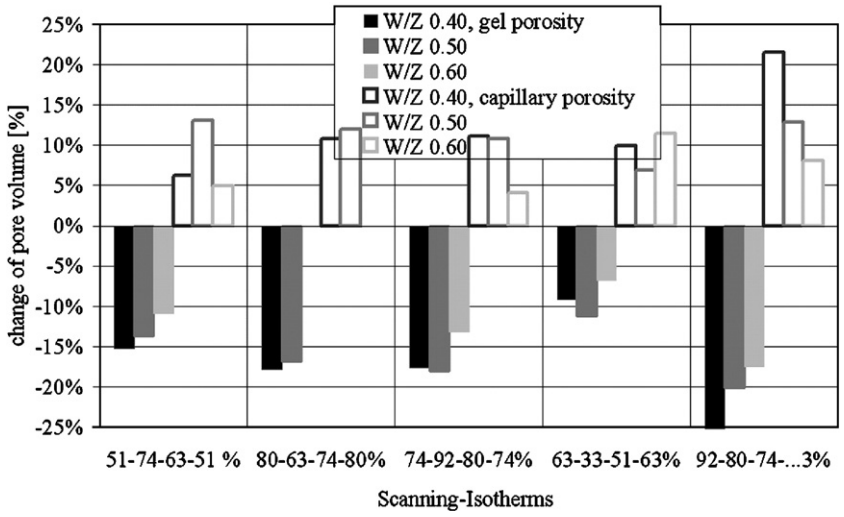

Fig. 21. Change of the gel and capillary pore volume of ZAB-28d measured by means of mercury intrusion porosimetry after storage by different humidity conditions.

depends on the amount and on the form of the inkbottle pores. Other researchers (i.e. [23,24]) consider also inkbottle pores as part of the pore structure of hardened cement paste.

The lower the vapour pressure is for drying the hardened cement paste, the coarser the pore structure becomes. The mercury intrusion porosimetry shows that the surface area becomes smaller while the average pore radius becomes larger. Moreover the total pore volume that can be measured (i.e. pore radius >1.8 nm) decreases slightly. However, the total pore volume (measured by means of water uptake) remains constant.

The chemical aging also causes a compaction of the cement gel. This explains the decrease of the measured pore surface area by means of the mercury intrusion porosimetry after chemical aging.

The cement hydration causes a change of the pore structure as the model of Powers predicts. Thus the amount of gel pores increases while the amount of capillary pores and the total pore volume decreases. The scaled hygroscopic water content contained in the gel pores yields another interesting result: the hygroscopic water content is directly proportional to the amount of hydrated hardened cement paste.

Otherwise, it has to be considered that for the calculation of the water content the dry weight of the sample also increases with the uptake of hydrate water.

Considering all these results it is now possible to describe mathematically the sorption behaviour in hardened cement paste at changing climatic conditions. This is the topic of a subsequent essay [15].

References

[1] J. Adolphs, M.J. Setzer, A model to describe sorption isotherms, Journal of Colloid and Interface Science 180 (1996) 70–76.

[2] J. Adolphs, M. J. Setzer, ESW—Eine neue Methode zur Auswertung von Sorptionsisothermen, GDCh-Monographie Band 7, Bauchemie, 1. Workshop, S.33 ff(1997).

[3] J. Adolphs, M.J. Setzer, Einfluβ der Feuchte auf die Mesoporenstruktur von Zementstein, Bauchemie, 178–180. GDCh-Monographie Band 11, Bauchemie-Tagung München 1997, S. 178–180 (1998).

[4] J. Adolphs, M.J. Setzer, P. Heine, Changes in pore structure and mercury contact angle of hardened cement paste depending on relative humidity, Materials and Structures 35 (2002) 477–486.

[6] P.W. Atkins, Physical Chemistry, Third edition, Oxford University Press, 1986.

[7] Z.P. Bazant, Thermodynamics of hintered sorption and its implications for hardened cement paste and concrete, Cement and Concrete Research 2 (1) (1972) S. 1–S. 16.

[8] J. Beaudoin, B. Tamtsia, Effect of drying methods on microstructural changes in hardened cement paste: an a.c. impedance spectroscopy evaluation, Journal of Advanced Concrete Technology 2 (1) (2004) 113–120.

[9] J.C.P. Broekhoff, Sorption and Capillarity, 1969.

[10] N.V. Chuarev, G. Starke, J. Adolphs, Isotherms of capillary condensation influenced by formation of a sorption films: 1. Calculation for model cylindrical and slit pores, Journal Colloid Interface and Interface Science 221 (2000) 246–253.

[12] B.V. Derjaguin, Theory of Stability of Colloids and Thin Films, 1989.

[14] R.M. Espinosa, Sorptionsisothermen von Zementstein und Mörtel, Dissertation Hamburg University of Technology, 2004.

[15] R.M. Espinosa, L. Franke, Inkbottle Pore-Method: prediction of hygroscopic water content in hardened cement paste at variable climatic conditions, Cement and Concrete Research 36 (2006) 1956–1970.

[16] R.F. Feldman, Sorption and length-change scanning-isotherms of methanol and water on hydrated Portland cement, Proceedings of the 5th International Congress on the Chemistry of Cement, vol. 3, Cement Association of Japan, Tokyo, 1968, pp. S. 53–S. 68.

[17] R.F. Feldman, P.J. Sereda, A model for hydrated Portland cement paste as deduced from sorption-length change and mechanical properties, Materiaux et Construction 1 (6) (1968) 509–520.

[18] Gätje, B. Nachträgliche Ermittlung betontechnologischer Parameter am Zementsteinen, Mörteln und Betonen unbekannter Zusammensetzung, Dissertation Technische Universität Hamburg-Harburg, 2003.

[19] J.W. Gibbs, The scientific papers of J. Willard Gibbs, Thermodynamics 1 (1993).

[20] S.J. Gregg, K.S.W. Sing, Sorption, Surface Area and Porosity, Academic Press, London, 1982.

[21] K.K. Hansen, Sorption Isotherms, A Catalogue, 1986.

[22] T.C. Hansen, Physical structure of hardened cement paste. A classical approach. Technical University of Denmark, Lyngby, Matériaux et Constructions, Vol. 19—No. 114, 423–436, 1986.

[23] Tetsuya Ishida, Rajesh Chaube, Toshiharu Kishi, Koichi Maekawa, Modeling of pore water content in concrete under generic drying–wetting conditions, Concrete library of JSCE, N 31 (1998) 275–287.

[24] Koichi Maekawa, Tetsuya Ishida, Toshiharu Kishi, Multi-scale modelling of concrete performance, Journal of Advanced Concrete Technology 1 (2) (2003) 91–126.

[25] I. Odler, Y. Chen, Investigations on the aging of hydrates tricalcium silicate and Portland cement pastes, Cement and Concrete Research 25 (5) (1995) 919–923.

[26] T.C. Powers, Properties of Cement Paste and Concrete. Paper V-1. Physical properties of Cement Paste, Proceedings of the Fourth International Symposium on the Chemistry of Cement, 1960.

[27] H. Schubert, Kapillarität in porösen Feststoffen, 1982.

[28] Setzer, M. J.: Oberflächenenergie und mechanische Eigenschaften des Zementsteins, Dissertation 1972, Technische Universität München.

[29] M.J. Setzer, Interaction of Water with Hardened Cement Paste, in: S. Mindess (Ed.), Ceramic Transactions: Advances in Cementitious Materials, vol. 16, American Ceramic Society, Westerville, OH, 1992, pp. 415–439.

[31] J. Stark, B. Möser, A. Eckart, Neue Ansätze zur Zementhydratation, ZKG international Nr. 1/2001 (Teil 1) und Nr. 2/2001 (Teil 2), Bauverlag, Springer Baumedien.

[32] J. Thomas, H. Jennings, Chemical Aging and the colloidal Structure of the CSH-Gel: Implications for creep and shrinkage, in Creep, Shrinkage and Durability Mechanics of Concrete and Other Quasi-Brittle Materials: Proceedings of the Sixth International Conference, Concreep-US-Ulm, F. J., Bazant, Zdenek P., Wittmann, Folker H. 2001/08 Pergamon Pr.

[33] J. Thomas, H. Jennings, A colloidal interpretation of chemical aging of the C-S-H gel and its effects on the properties of cement paste, Cement and Concrete Research 36 (1) (2006) 30–38.

[34] F.H. Wittmann, Interaction of hardened cement paste and water, Journal of American Ceramics Society 56 (8) (1973) 409–415.

[35] F.H. Wittmann, Drying and Shrinkage of Hardened Cement Paste, Pore Solution in Hardened Cement Paste, Aedificatio Publishers, Freiburg, 2000.

[36] H.M. Jennings, A model for the microstructure of calcium silicate hydrate in cement paste, Cement and Concrete Research 36 (2000) 101–116.